GEOPHYSICAL RESEARCH LETTERS, VOL. 26, NO. 8, PAGES 1015-1018, APRIL 15, 1999

A numerical investigation of the spring Ross Sea polynya

T. Fichefet and H. Goosse
Institut d'Astronomie et de Géophysique G. Lemaître, Université Catholique de Louvain, Louvain-la-Neuve, Belgium

Abstract. In November and December, a polynya (area of reduced ice concentration surrounded by heavy pack ice) usually develops on the western Ross Sea continental shelf immediately north of the Ross Ice Shelf. This important regional feature is reasonably well simulated by the Université Catholique de Louvain (UCL) global ice-ocean model, despite its coarse resolution. The model results suggest that both the wind-induced divergence of the sea ice and the inflow of relatively warm Circumpolar Deep Water (CDW) onto the continental shelf are essential for the polynya formation, which supports the inference drawn from observational data.

1. Introduction

At predictable, recurrent locations throughout the polar regions, there are oceanic areas that remain partially or totally ice-free at times and under meteorological conditions where the water is expected to be ice-covered. These features, termed polynyas, range in area from hundreds to hundreds of thousands square kilometers. They can form by two mechanisms: (1) a divergence in the sea ice drift, which gives rise to an import of latent heat into the area, and (2) an influx of oceanic heat into the local region preventing ice formation or melting the ice. The first mechanism creates polynyas referred to as latent heat polynyas, and the second one creates sensible heat polynyas. These two mechanisms are not mutually exclusive, and in many cases, both contribute to the polynya maintenance [*Smith et al.*, 1990].

Such a polynya is observed in November and December on the western Ross Sea continental shelf [see, e.g., *Zwally et al.*, 1985; *Gloersen et al.*, 1992]. The presence of this wide area of low ice concentration within the Ross Sea ice pack at the beginning of the melt season has two important consequences. First, the polynya admits large quantities of solar radiation to the upper ocean which ultimately affect the mass balance of the surrounding ice cover [*Jacobs et al.*, 1970]. Second, the availability of light and nutrients inside the polynya allows the development of an intense phytoplankton bloom that contributes significantly to the global oceanic uptake of atmospheric CO_2 [e.g., *Bates et al.*, 1998].

Several lines of evidence suggest that this spring Ross Sea polynya is caused by strong offshore winds moving the sea ice out of the area and by intrusions of relatively warm water from the continental slope region melting the ice [*Jacobs and Comiso*, 1989]. Here we show that the results from a global, coarse-resolution ice-ocean model are consistent with this hypothesis.

Paper number 1999GL900159.
0094-8276/99/1999GL900159$05.00

2. Model description

Apart from the inclusion of a more physical formulation of the subgrid-scale oceanic vertical mixing (the *Kantha and Clayson* [1994] version of the *Mellor and Yamada* [1982] level-2.5 turbulence closure scheme; H. Goosse et al., Sensitivity of a global ocean–sea ice model to the parameterization of vertical mixing, submitted to *Journal of Geophysical Research*, 1998) and a parameterization of density-driven downslope flows [*Campin and Goosse*, 1999], the model used in this study is identical to that of *Goosse et al.* [1997a; 1997b]. It is made up of a primitive-equation, free-surface ocean general circulation model coupled to a thermodynamic-dynamic sea ice model with viscous-plastic rheology. The horizontal resolution is of $3° \times 3°$, and there are 20 unequally spaced vertical levels in the ocean. The bathymetry is a discretized version of the real World Ocean bottom topography.

The model is dynamically driven by the climatological monthly wind stresses of *Hellerman and Rosenstein* [1983] between 15°N and 15°S and of *Trenberth et al.* [1989] out of this region. The surface fluxes of heat are determined from atmospheric data by using classical bulk formulas. Input fields consist of climatological monthly surface air temperatures [*Taljaard et al.*, 1969; *Crutcher and Meserve*, 1970] and relative humidities [*Trenberth et al.*, 1989], cloud fractions [*Berliand and Strokina*, 1980], and surface winds (same sources as for wind stresses). Evaporation/sublimation is derived from the turbulent flux of latent heat. Precipitation and freshwater inflow from the largest rivers are prescribed according to the monthly climatologies of *Xie and Arkin* [1996] and *Grabs et al.* [1996], respectively. For the smaller rivers, the annual runoff values of *Baumgartner and Reichel* [1975] are utilized. In addition to this forcing, a relaxation toward observed annual mean salinities [*Levitus*, 1982] is applied in the 10-m-thick surface grid box with a time constant of 2 months. This weak restoring circumvents the surface salinity drift that would occur through the lack of any stabilizing feedback if the ocean is forced with slightly incorrect evaporation, precipitation, and runoff fields.

The spin-up procedure is the following. The model is first integrated for 20 years in robust diagnostic mode (i.e., with interior restoring to the annual mean Levitus temperatures and salinities on a 1-year time scale) from a state of rest with no ice and horizontally uniform profiles of temperature and salinity. The relaxation is then

suppressed, except in the uppermost grid box for salinity (see above), and the integration is pursued for 1000 years. At the end of this phase, a quasi-equilibrium state is achieved, the trends in temperature and salinity at the lowest model level (depth of 5125 m) being less than 2.5×10^{-3} °C per century and 2×10^{-3} psu per century, respectively. All results discussed below are averages over the last 10 years of integration.

3. Results and Discussion

Despite its coarse resolution, the model is capable of producing a reasonable simulation of the springtime and summertime sea ice characteristics in the Ross Sea sector (Figure 1). In November, the modeled ice cover is generally less compact above the continental shelf than over the adjacent deep ocean. In mid-December, the ice concentration drops below 0.50 in the western Ross Sea immediately north of the ice shelf front, which is indicative of a polynya formation. The polynya then expands rapidly to the north, and at the end of January, it joins the outer ice edge that gradually retreats southward. By February, the western side of the Ross Sea is essentially ice-free, while the eastern side remains to a large extent ice-covered. This pattern of ice decay corresponds qualitatively with that of sea ice climatologies derived from satellite passive-microwave observations [e.g., *Sturman and Anderson*, 1986; *Gloersen et al.*, 1992]. However, in the real world, the Ross Sea polynya begins to form about one month earlier [*Arrigo et al.*, 1998]. Furthermore, it extends less far west and farther east than in the model, which leads to a more pronounced shrinkage of the eastern Ross Sea ice cover during summer months [see *Gloersen et al.*, 1992].

Figure 2 shows the seasonal cycles of the gain/loss of ice by advection in the lettered grid cells in Figure 1a. It can be seen that sea ice is continuously removed from the southern coastal region (grid cells A and C) during the cold season. The ice export is particularly large on the western shelf (grid cell A), with ice losses of up to 2.5 cm per day. This strong divergence is for the most part induced by the intense southerly winds prevailing in this area at that time. In December, there is an import of ice into grid cell C, whereas ice continues to be extracted from grid cell A. In grid cell B, which is located north of grid cell A in a deep oceanic region, ice divergence alternates with ice convergence throughout the year. As the polynya enlarges, less and less ice enters grid cell B from the south. By January, the ice supply has become much weaker than the ice outflow taking place at the northern boundary of the grid cell, resulting in an ice loss of as much as 2 cm per day.

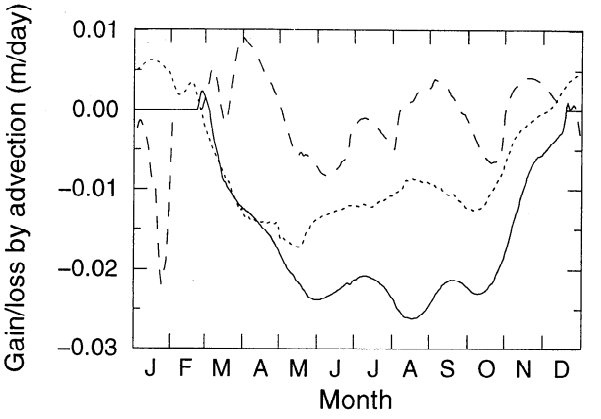

Figure 2. Seasonal variations of the gain/loss of ice by advection in grid cells A (full line), B (dashed line), and C (dotted line). See Figure 1a for the locations of these grid cells.

Figure 3 displays the spatial variations of the sensible heat flux from the ocean to the ice in the Ross Sea region at the time of the maximum ice coverage. Values

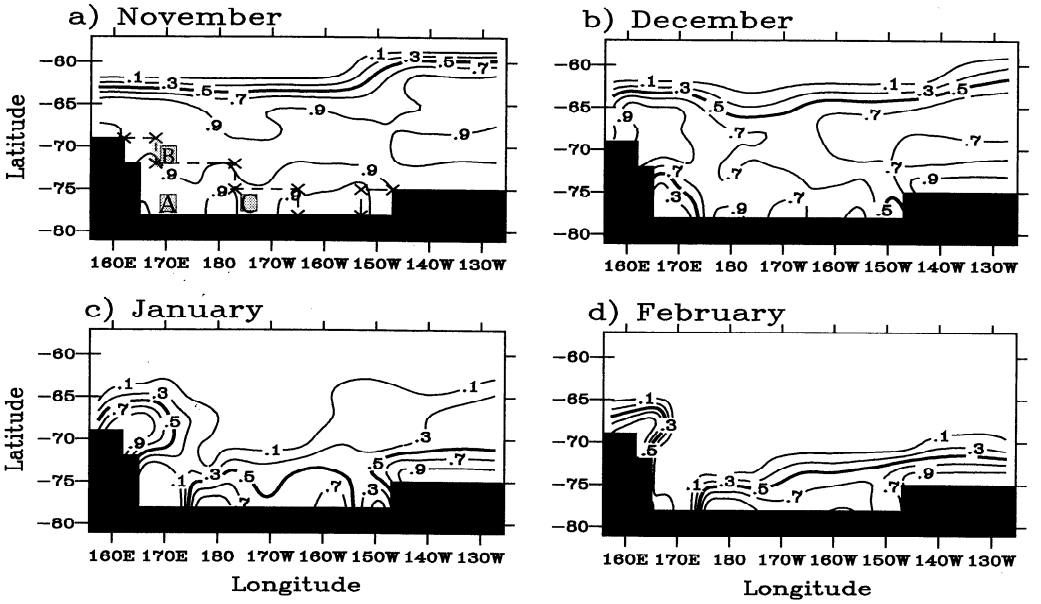

Figure 1. Monthly average sea ice concentrations in the Ross Sea sector from the model reference run for November (a), December (b), January (c), and February (d). Contour interval is 0.20. The northern limit of the model continental shelf (depth less than 1000 m) is indicated by a dashed line in Figure 1a. Lettered grid cells in this figure denote locations of more detailed analysis.

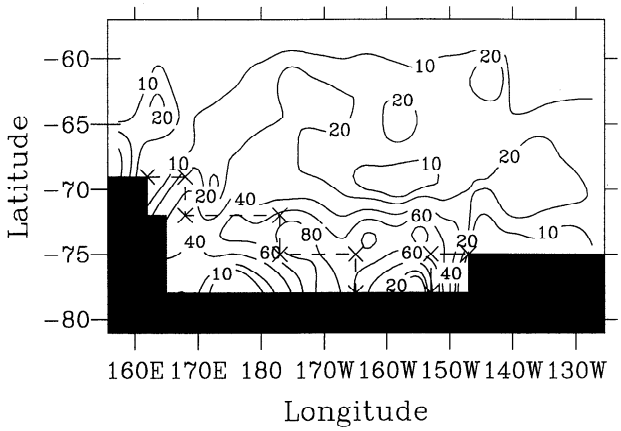

Figure 3. Monthly average values of the oceanic heat flux in the Ross Sea sector from the model reference run for September. Selected contours are 10, 20, 40, 60, and 80 W m^{-2}. The northern limit of the model continental shelf (depth less than 1000 m) is indicated by a dashed line.

greater than 60 W m^{-2} are noticed at the continental shelf break and in some areas of the shelf. These values are by far the largest on the model Antarctic continental shelf. In fact, relatively warm CDW flows in southward in mid-depth tongues (Figure 4). Such inflows occur at other places along Antarctica in the model (e.g., in the Bellingshausen Sea). However, in the Ross Sea, the heat is efficiently transferred to the near-surface layers by upward advection and by the vigorous vertical mixing driven by brine rejection during sea ice formation, thus yielding a high oceanic heat flux at the bottom of the ice. In addition to these warm, seasonally persistent intrusions at intermediate depths, the model simulates a bottom off-shelf flow of cold (and therefore dense) water year-round (see Figure 4). This export, which is carried out by the large-scale currents resolved by the model and by the parameterized downslope currents, contributes to the production of Antarctic Bottom Water. It should be noted that the model does fairly well in simulating the characteristics of this water mass [*Goosse et al.*, 1997b].

The large oceanic heat flux combines with the strong ice export to prevent winter ice concentration and thickness in the southern Ross Sea from exceeding 0.90 and 1 m, respectively, in accordance with observational estimates [e.g., *Jacobs and Comiso*, 1989; *Jeffries and Adolphs*, 1997]. On the western shelf, this weak ice cover is easily withdrawn in late spring through advection and local melting. Among these two processes, the first one is the most efficient. In grid cell A, for instance, only 40% (i.e., ~35 cm) of the ice mass present at the end of the cold season melts locally. The oceanic heat flux, which amounts to 15–20 W m^{-2} during this period, contributes 40% to this melting, the remainder being mainly due to the solar radiation absorbed in the low-albedo leads. Once open, the polynya swiftly increases in area as both processes continue to act. The conditions are very different on the eastern shelf. As mentioned above, ice is generally imported into this region in late spring and early summer. So, even if the local melting is somewhat stronger than on the western shelf, the ice cover never totally disappears.

In order to further illustrate the importance of the ice transport and of the flux of sensible heat at the ice-ocean interface for the polynya formation, two sensitivity experiments were conducted with the model. In the first one, ice dynamics was not taken into account, while in the second one, no exchange of salt or freshwater between ice and ocean was allowed over the entire model domain. As expected, no polynya develops when sea ice is kept motionless. When the salt/freshwater flux associated with ice freezing/melting is omitted, minimum ice concentrations of ~0.60 are simulated in the southwestern Ross Sea during summer. In this experiment, the ice velocities are nearly identical to those of the reference run. However, the oceanic heat flux at the bottom of the ice drops to less than 5 W m^{-2} in the continental shelf area at the time of the maximum ice extent. Two main effects contribute to this decrease. First, as no brine is rejected from the growing sea ice, the turbulent activity in the mixed layer weakens, and thus less heat from the deeper layers is entrained into this layer. Second, the subsurface inflow of relatively warm water is significantly reduced. This reduction is partly caused by the strong decrease in density observed on the shelf: the lighter shelf bottom waters no longer flow out of the shelf, which gives rise, by continuity, to a weakening of the CDW intrusions.

4. Conlusions

The UCL global ice-ocean model reproduces rather well the main features that dominate the large-scale ice compactness and thickness in the Ross Sea. Of particular interest in the reference experiment is the appearance of a polynya in the same geographical area as the observed spring Ross Sea polynya. The model results suggest that both the wind-induced divergence of the ice pack and the transfer to the surface of relatively warm water originating from the Antarctic Circumpolar Current are crucial for the polynya opening. This supports the conclusion reached by *Jacobs and Comiso* [1989] on the basis of observational data.

Quantitatively, there are differences between the observed and computed sea ice concentrations. For instance, the polynya forms about one month too late in the model, it expands too far westward, and too much ice remains in the eastern Ross Sea in summer. These errors are partially attributable to the coarse resolution of the model and to the absence of daily variabil-

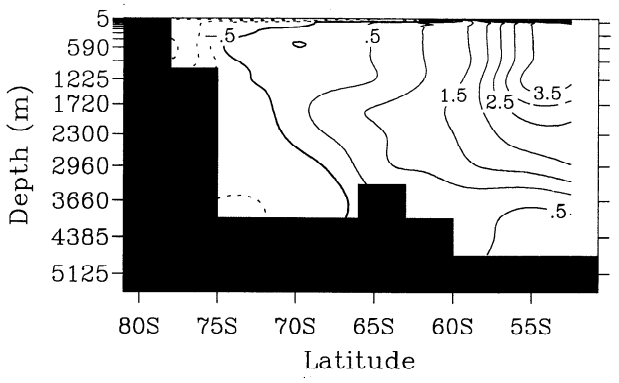

Figure 4. Vertical section of annual mean potential temperature along 167°W in the model Southern Ocean and Ross Sea. Contour interval is 0.5°C.

ity in the atmospheric forcing used. Furthermore, it should be mentioned that the model does not account for the interactions between the Ross Ice Shelf and the ocean. As those interactions seem to play a role in setting the properties of the shelf bottom waters [*Jacobs et al.*, 1985], they might also impact on the polynya formation. Finally, note that, owing to its coarse horizontal mesh, the model cannot resolve the small-scale polynyas that exist throughout winter in many places along the Antarctic coastline (including the Ross Sea) [e.g., *Zwally et al.*, 1985; *Bromwich et al.*, 1998]. In spite of these shortcomings, it is encouraging that a model utilized in global climate studies is able to simulate naturally occurring regional features such as the spring Ross Sea polynya.

Acknowledgments. We thank J.-M. Campin and B. Tartinville for their help in the preparation of the figures and the three anonymous referees for their careful reading of the manuscript and constructive criticism. Both of us are sponsored by the National Fund for Scientific Research (Belgium). This work was done within the scope of the Global Change and Sustainable Development Programme (Belgian State, Prime Minister's Services, Federal Office for Scientific, Technical, and Cultural Affairs, contract CG/DD/09A) and the Concerted Research Action 097/02-208 (French Community of Belgium, Department of Education, Research, and Formation). All of this support is gratefully acknowledged.

References

Arrigo, K. R., A. M. Weiss, and W. O. Smith Jr., Physical forcing of phytoplankton dynamics in the southwestern Ross Sea, *J. Geophys. Res.*, *103*, 1007–1021, 1998.

Bates, N. R., D. A. Hansell, C. A. Carlson, and L. I. Gordon, Distribution of CO_2 species, estimates of net community production, and air-sea CO_2 exchange in the Ross Sea polynya, *J. Geophys. Res.*, *103*, 2883–2896, 1998.

Baumgartner, A., and E. Reichel, *The World Water Balance*, 179 pp., Elsevier, New York, 1975.

Berliand, M. E., and T. G. Strokina, *Global Distribution of the Total Amount of Clouds* (in Russian), 71 pp., Hydrometeorological, Leningrad, Russia, 1980.

Bromwich, D. H., Z. Liu, A. N. Rogers, and M. L. Van Woert, Winter atmospheric forcing of the Ross Sea polynya, in *Ocean, Ice, and Atmosphere: Interactions at the Antarctic Continental Margin, Antarc. Res. Ser.*, vol. 75, edited by S. S. Jacobs and R. F. Weiss, pp. 101–133, AGU, Washington, D. C., 1998.

Campin, J.-M., and H. Goosse, A parameterization of density-driven downsloping flow for a coarse-resolution ocean model in z-coordinate, *Tellus*, in press, 1999.

Crutcher, H. L., and J. M. Meserve, Selected level heights, temperatures and dew points for the Northern Hemisphere, *NAVAIR Rep. 50-1C-52*, revised, U. S. Nav. Weather Serv. Command, Washington, D. C., 1970.

Gloersen, P., W. J. Campbell, D. J. Cavalieri, J. C. Comiso, C. L. Parkinson, and H. J. Zwally, Arctic and Antarctic sea ice, 1978–1987: Satellite passive-microwave observations and analysis, *NASA Spec. Publ.*, *SP–511*, 290 pp., 1992.

Goosse, H., J.-M. Campin, T. Fichefet, and E. Deleersnijder, Sensitivity of a global ice–ocean model to the Bering Strait throughflow, *Clim. Dyn.*, *13*, 349–358, 1997a.

Goosse, H., J.-M. Campin, T. Fichefet, and E. Deleersnijder, Impact of sea-ice formation on the properties of Antarctic Bottom Water, *Ann. Glaciol.*, *25*, 276–281, 1997b.

Grabs, W., T. De Couet, and J. Pauler, Freshwater fluxes from continents into the world oceans based on data of the global runoff data base, *Global Runoff Data Centre Rep. 10*, 228 pp., Fed. Inst. of Hydrol., Koblenz, Germany, 1996.

Hellerman, S., and M. Rosenstein, Normal monthly wind stress over the World Ocean with error estimates, *J. Phys. Oceanogr.*, *13*, 1093–1104, 1983.

Jacobs, S. S., and J. C. Comiso, Sea ice and oceanic processes on the Ross Sea continental shelf, *J. Geophys. Res.*, *94*, 18,195–18,211, 1989.

Jacobs, S. S., A. F. Amos, and P. M. Bruchhausen, Ross Sea oceanography and Antarctic Bottom Water formation, *Deep-Sea Res.*, *17*, 935–962, 1970.

Jacobs, S. S., R. Fairbanks, and Y. Horibe, Origin and evolution of water masses near the Antarctic continental margin: Evidence from $H_2{}^{18}O/H_2{}^{16}O$ ratios in seawater, in *Oceanology of the Antarctic Continental Shelf, Antarc. Res. Ser.*, vol. 43, edited by S. Jacobs, pp. 59–85, AGU, Washington, D. C., 1985.

Jeffries, M. O., and U. Adolphs, Early winter ice and snow thickness distribution, ice structure and development of the western Ross Sea pack ice between the ice edge and the Ross Ice Shelf, *Antarct. Sci.*, *9*, 188–200, 1997.

Kantha, L. H., and C. A. Clayson, An improved mixed layer model for geophysical applications, *J. Geophys. Res.*, *99*, 25,235–25,266, 1994.

Levitus, S., Climatological atlas of the World Ocean, *NOAA Prof. Pap. 13*, 173 pp., U. S. Gov. Print. Office, Washington, D. C., 1982.

Mellor, G. L., and T. Yamada, Development of a turbulence closure model for geophysical fluid problems, *Rev. Geophys. Space Phys.*, *204*, 851–875, 1982.

Smith, S. D., R. D. Muench, and C. H. Pease, Polynyas and leads: An overview of physical processes and environment, *J. Geophys. Res.*, *95*, 9461–9479, 1990.

Sturman, A. P., and M. R. Anderson, On the sea-ice regime of the Ross Sea, Antarctica, *J. Glaciol.*, *32*, 54–59, 1986.

Taljaard, J. J., H. van Loon, H. L. Crutcher, and R. L. Jenne, Climate of the upper air, I, Southern Hemisphere, vol. 1, Temperatures, dew points, and heights at selected pressure levels, *NAVAIR Rep. 50-1C-55*, 135 pp., U. S. Nav. Weather Serv. Command, Washington, D. C., 1969.

Trenberth, K. E., J. G. Olson, and W. G. Large, A global ocean wind stress climatology based on ECMWF analyses, *National Center for Atmos. Res. Tech. Note, NCAR/TN-338+STR*, 93 pp., 1989.

Xie, P., and P. A. Arkin, Analyses of global monthly precipitation using gauge observations, satellite estimates and numerical model predictions, *J. Clim.*, *9*, 840–858, 1996.

Zwally, H. J., J. C. Comiso, and A. L. Gordon, Antarctic offshore leads and polynyas and oceanographic effects, in *Oceanology of the Antarctic Continental Shelf, Antarc. Res. Ser.*, vol. 43, edited by S. Jacobs, pp. 203–226, AGU, Washington, D. C., 1985.

T. Fichefet and H. Goosse, Institut d'Astronomie et de Géophysique G. Lemaître, Université Catholique de Louvain, B-1348 Louvain-la-Neuve, Belgium, (e-mail: fichefet@astr.ucl.ac.be; hgs@astr.ucl.ac.be)

(Received September 25, 1998; revised January 18, 1999; accepted February 22, 1999.)